A Case Study of Bolt Performance in a Two-entry Gateroad

Stephen P. Signer, Mining Engineer

National Institute for Occupational Safety and Health
Spokane Research Center
Spokane, WA

John L. Lewis, Mining Engineer

Energy West Mining Company
Huntington, UT

ABSTRACT

This paper presents the results of a case study conducted in a two-entry gateroad in a coal mine where excessive roof deformation and bolt loading resulted in failure of many roof supports. The instruments consisted of 16 fully grouted, strain-gaged resin bolts, load cells on both full and partially grouted cable bolts, and vertical deflection multipoint extensometers. These instruments were installed on-cycle to measure loading on bolts in an existing support pattern and to determine if cable bolts could be used to improve roof stability.

Results showed significant amounts of movement within the bolted zone. In some cases, these movements were enough to load the supports past their ultimate strength. Geology appeared to be a significant factor in localized roof degradation; that is, a very weak rock layer in the immediate roof overlain by a very strong rock layer contributed to the development of shear planes.

Only one instrumented bolt had a maximum strain of less than 2,000 microstrain, which was the yield point of the steel. The average maximum strain on all bolts was 20,000 microstrain. However, electrical continuity to many gages was lost, and a pattern was noted that would indicate possible bolt failure. Wire mesh and concrete cans installed as secondary support performed very effectively.

INTRODUCTION

Millions of roof bolts are installed in U.S. mines each year. Many of these supports fail, resulting in more than 400 injuries and 10 fatalities a year. Despite the importance of entry stability, there are no adequate methods to relate roof bolt loads, diameter, length, and spacing to mining conditions such as geology, geometry, and in situ stress fields. The Spokane Research Laboratory (SRL), a division of the National Institute for Occupational Safety and Health (NIOSH), is conducting research on roof bolt loading to reduce support failure and subsequent ground falls.

Fully grouted roof bolts have become the primary support in underground coal mines. This type of support responds to rock movements, which results in a nonlinear distribution of load along the length of the bolt. Previous laboratory and field studies (*1-10*) have shown that strain gages can be used to measure both axial and bending loads on each bolt in the pattern, where loads are being developed, and how much anchorage length is available to provide support. Such information can be very useful in establishing safe support patterns for various mining conditions.

Excessive roof deformation and bolt loading were occurring in several gateroad entries at the Trail Mountain Mine near Orangeville, UT. The problem areas were located in a two-entry development where entry widths were approximately 6 m (20 ft). Pillars were spaced on 15- by 31-m (50- by 100-ft) centers. The coal seam was 3 to 3.4 m (10 to 11 ft) thick and was mined to a height of approximately 2.4 to 2.7 m (8 to 9 ft). Overburden thickness was 427 to 487 m (1,400 to 1,600 ft). The primary roof support was 2.1-m (7-ft), No. 6, grade-60 fully grouted bolts that were spaced approximately 1.5 m (5 ft) across the entry and 1.5 m (5 ft) along the entry. Wire mesh and roof mats were also installed. Secondary support consisted of two rows of 0.9-m (3-ft) diameter can cribs spaced approximately 2 m (7 ft) on center down the entry with a 1.2- to 2.4-m (4- to 6-ft) wide walkway down the middle. The cribs were installed approximately 30 m (100 ft) ahead of the longwall face.

Geology may have been a significant factor in the localized roof degradation. Several 2.7- to 4.6-m (9- to 15-ft) deep core-holes were drilled, and AX core was removed and tested to assist in a geological assessment of the roof. The immediate roof in the bad areas had layers of very weak mudstone, carbonaceous mudstone, and coal. Immediately above these weak layers was a very strong siltstone-sandstone member that had an average compressive strength of 179 MPa (24,600 psi). The mudstone was too weak to allow recovery of a sample large enough to test. The core log near crosscut 59.5 is shown in figure 1.

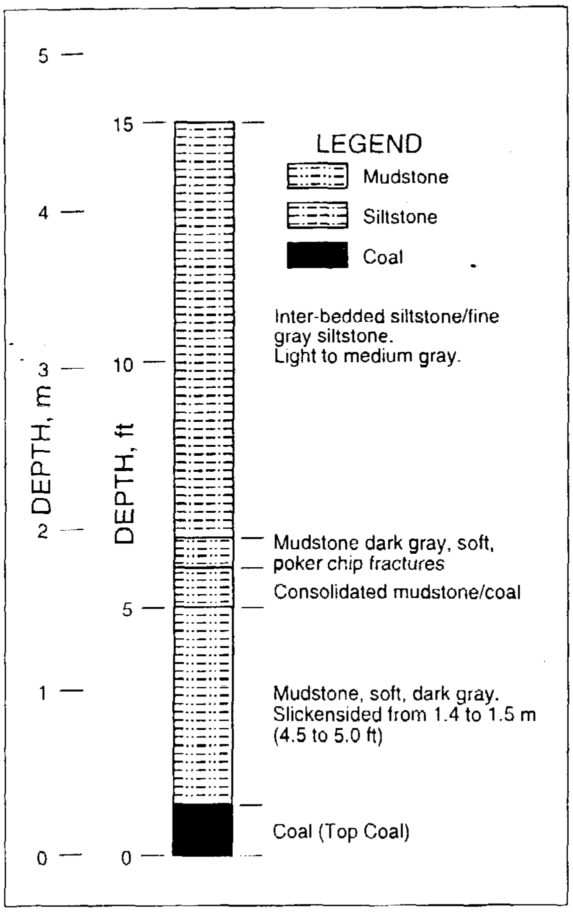

Figure 1.—Core log near crosscut 59

Sixteen instrumented, fully grouted bolts, as well as sagmeters and pressure pads, were installed on-cycle in three test areas in the 10th Right gateroad to measure loading on bolts in the existing support pattern and to determine if cable bolts could be used to improve roof stability. This gateroad was the last in a sequence of longwall panels (figure 2).

TEST AREAS

In the first test area, a combination of fully grouted cable bolts and resin bolts was used (table 1). Two rows of instruments were located approximately 12 m (40 ft) outby from the center of crosscut 62. The resin bolts and cable bolts were alternated as shown in figure 3*A*.

In the second test area, a combination of partly grouted cable bolts and resin bolts was used (table 1). Two rows of instruments were located approximately 8 m (27 ft) inby from the center of crosscut 62 (figure 3*B*).

Two rows of instrumented No. 7, grade-60, 6-ft-long resin bolts were installed in the third test area as the primary support. The first row was 4.9 m (16 ft) inby the center of crosscut 56, and the second row was 19.8 m (65 ft) inby the center of crosscut 56 (figure 3*C-D*). The connector to an instrumented bolt in this test area was severed during installation. The uninstrumented resin bolts were 2.1-m (7-ft) long and were No. 6, grade 60. Entry development and longwall pass of the test rows are shown in table 2. This gateroad had only one longwall panel pass.

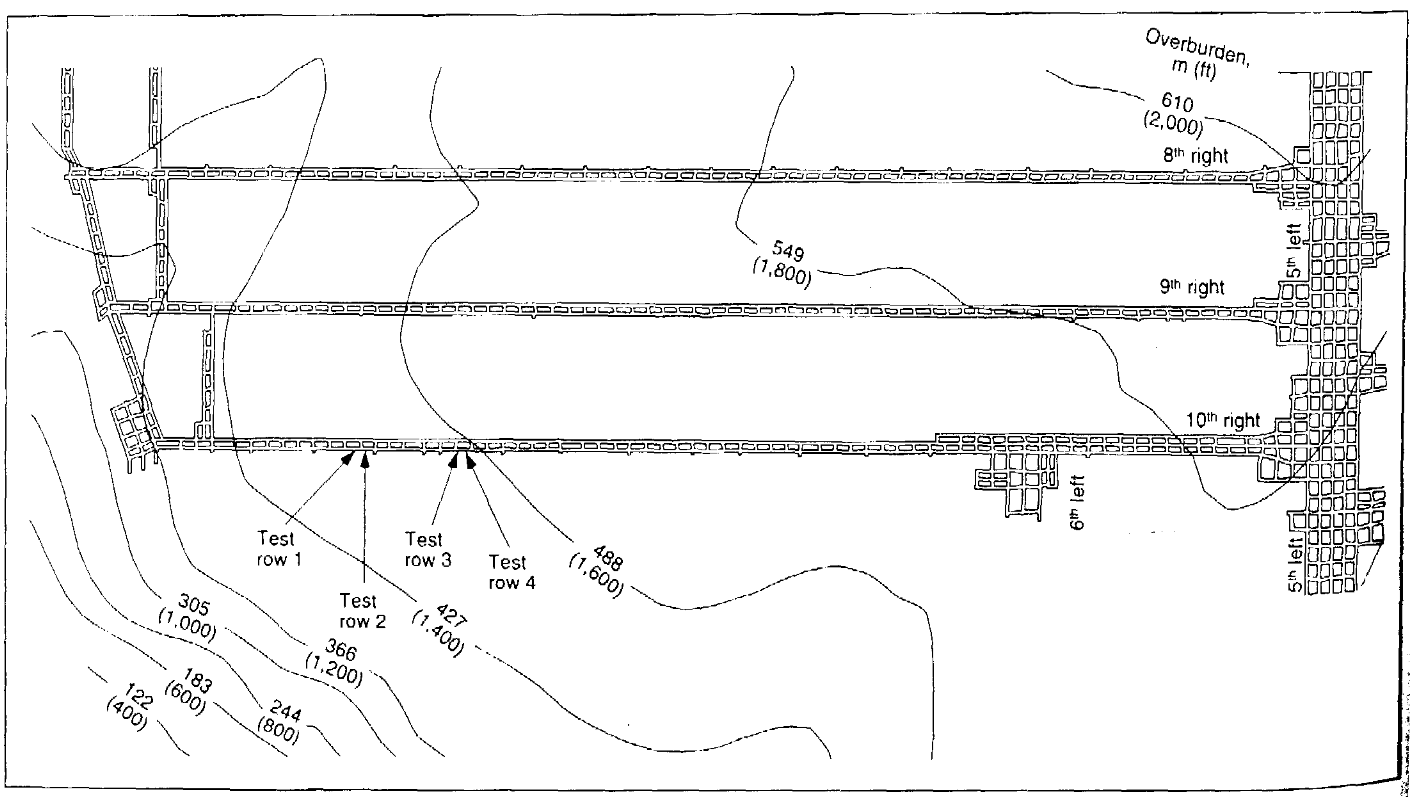

Figure 2.—Plan view of test areas

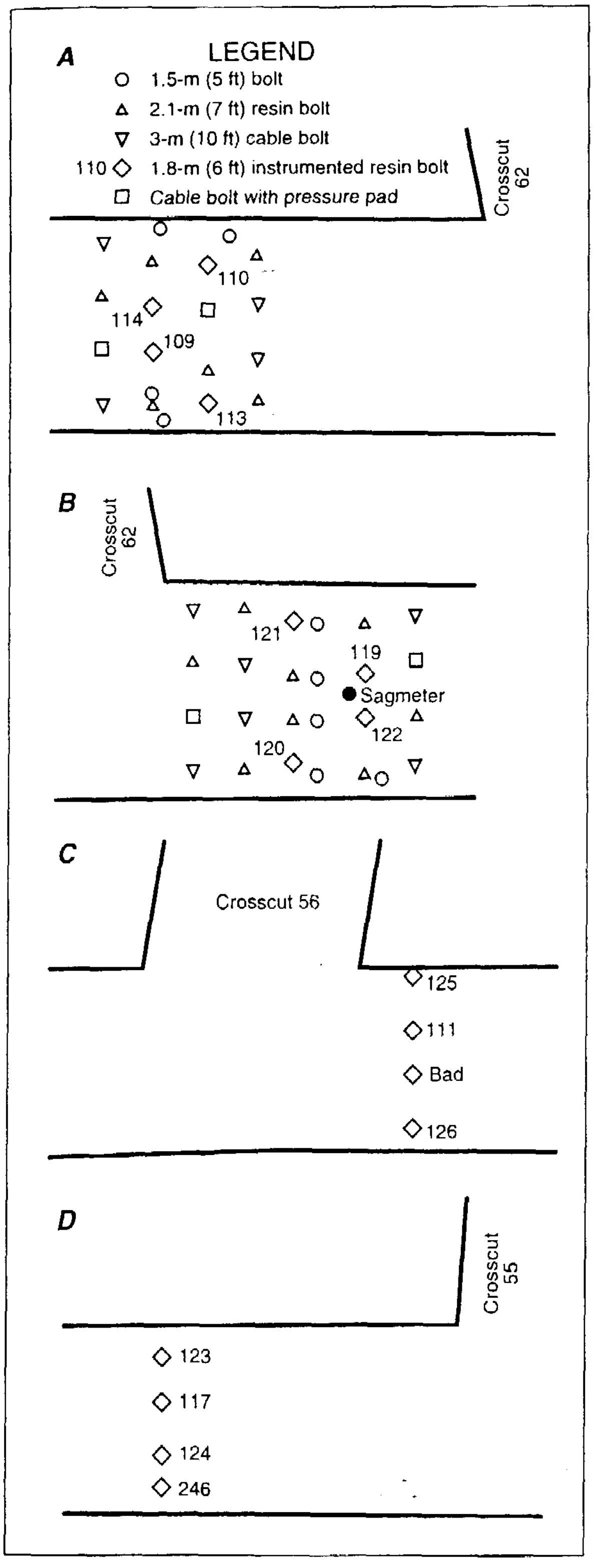

Figure 3.—Test rows. *A*, Fully grouted bolts; *B*, partly grouted bolts; *C*, resin bolts, row 3; *D*, resin bolts, row 4.

Table 1.—Description of cable bolts in test rows 1 and 2

	Length	Resin length	Diameter	Ultimate strength
Test row 1:	3 m	2.7 m	18 mm	356 kN
	10 ft	9 ft	0.7 in	80,000 lb
Test row 2:	3 m	1.5	15 mm	267 kN
	10 ft	5 ft	0.6 in	60,000 lb

Table 2.—Significant dates of test rows.

Test row	Developed	Cribs installed	Longwall pass
1	12/10/97	4/16/98	4/21/98
2	12/9/97	4/18/98	4/22/98
3	12/1/97	5/17/98	5/19/98
4	12/1/97	5/18/98	5/20/98

INSTRUMENTS

The resin bolts were modified by milling a slot 6.4 mm (1/4 in) wide and 3.2 mm (1/8 in) deep. Five strain gages were attached on both sides, as shown in figure 4. Because these bolts were used for primary support, No. 7 bolts were used in place of the No. 6 bolts. Table 3 describes the properties of the two bolts. Note that the No. 7 bolt has an increased capacity of approximately 28%.

Table 3.—Properties of bolts

Bolt type	Yield load	Ultimate load	Cross-sectional area
No. 6	107 kN	176 kN	2.58 cm^2
	24,000 lb	39,500 lb	0.40 in^2
No. 7, slotted	149 kN	249 kN	3.61 cm^2
	33,500 lb	55,900 lb	0.56 in^2

An Omnidata Polyrecorder data acquisition system (DAS) was used to measure load on the instrumented bolts. Readings were taken immediately after installation and then periodically as mining-induced stresses changed. The strain gages on the bolts were wired into a Wheatstone bridge configuration using 350-ohm resistors and a 5-V excitation. The accuracy of the system is ±0.445 kN (100 lb).

Loads on the cable bolts were measured on a 64.5 cm^2 (10-in^2) bearing plate with hydraulic pressure cells. Vertical roof movements were measured with multipoint extensometers with anchors set at depths of 4.3, 3, 1.8, and 0.9 m (14, 10, 6, and 3 ft) from the roofline.

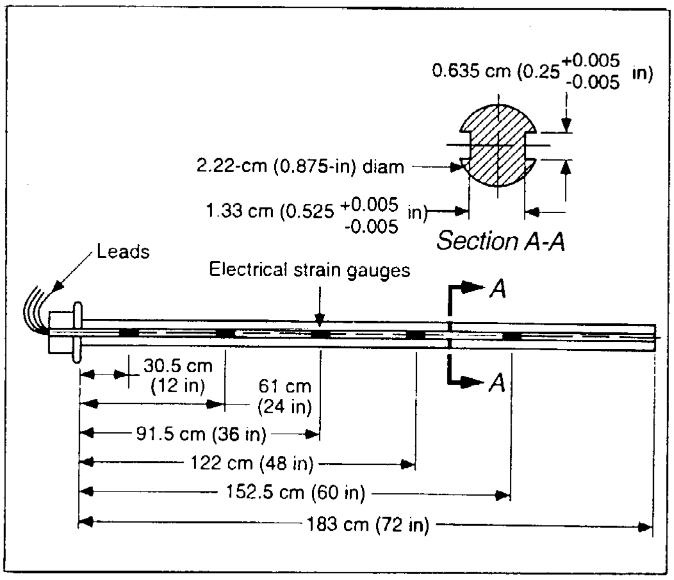

Figure 4.—Instrumented bolt

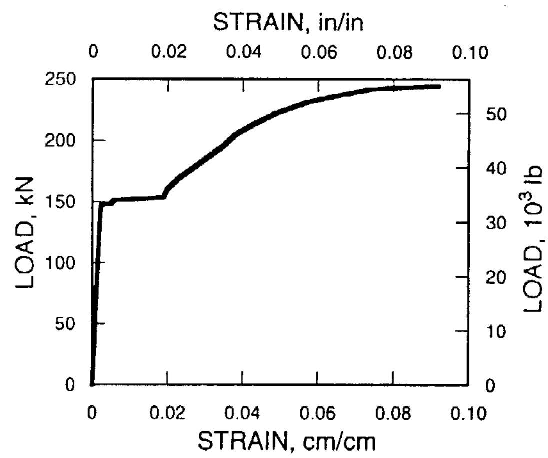

Figure 5.—Load strain plot for No. 7, grade 60, slotted bolt

TYPES OF BOLT LOADS

Bolt loads can be axial, bending, and/or shear. Axial loading is generally the primary force on a steel bolt, although under some situations, combinations of axial, bending, and/or shear forces can cause bolt failure. Shear loads are impossible to estimate with this type of instrument because of the nature of the loading mechanisms and uncertainties in determining the point of loading. However, when joint movement is present, shear loading can be critical in the design of bolt systems, and additional research is required for a better understanding of this loading mechanism.

A design engineer should consider several factors when calculating bending moments measured by instrumented bolts. Maximum bending moments may be localized and not measured accurately. Bending is measured in only one plane, but can take place in other directions, especially if high horizontal stress fields are present. (At our test sites, bolts were oriented during installation to measure the highest estimated plane of bending.) Bending moments can also be caused by joint movement, large-block rotations, and/or differential loading in mats and meshes.

Another, equally important, aspect of selecting bolts for roof support is the evaluation of strain levels in the bolt (figure 5). Typical engineering design limits strain to a percentage of the yield point. Previous evaluations of strain measured on roof bolts show that, in many cases, the yield point of the steel bolt is exceeded where the roof remains stable. Fully grouted roof bolts are a stiff support system in which loads increase quickly as the bolted strata move. Rebar bolts are made from a ductile steel that can reach strain levels of 100,000 to 160,000 microstrain at ultimate load. Yielding occurs at approximately 2,000 microstrain on grade 60 rebar. Immediately after yielding, the bolt will continue to stretch, with very little increase in load until the steel begins to work harden. Thus, design strain limits should take bolt loading mechanisms (i.e., axial, bending, and/or shear) into consideration. Bolts loaded axially with little bending or shear load can reach higher strain levels than bolts subjected to high shear and bending forces.

Data from each instrumented bolt were evaluated in several different ways. Each bolt was calibrated in a uniaxial testing machine to correlate voltage change to load change. This calibration factor was used below the steel yield point to convert voltage data to load at each of the 10 strain gages. If a bolt section exceeded the steel yield point, the strain was calculated and load estimated from the stress-strain relationship shown in figure 5.

Axial loading was calculated by averaging the load on each side of the bolt at each gage location. Bending moment was calculated with standard beam equations. The section modulus used to calculate bending was determined both experimentally and mathematically. If a strain gage fails, then neither axial load nor bending moment can be calculated for that bolt location. Strain was calculated directly from the voltage readings based on the equation—

$$\epsilon = \frac{4\,\Delta V}{(GF)(EV)}$$

where ϵ = strain, in/in,
ΔV = change, V,
GF = gage factor,
and EV = excitation voltage.

RESULTS

Bolt loading is shown in figures 6 through 22 as a cross-sectional view. Each test row is shown at various time intervals. Figures 6 through 13 show the development of axial loading in the row of fully grouted cable bolts. On December 12, gage 4 on bolt 114 had reached 43,000 microstrain, well into the strain-hardening phase of the steel. When that bolt was read again 4 days later, that gage had an open reading and axial loading on the adjacent bolts had increased. Three weeks later, the strain gage

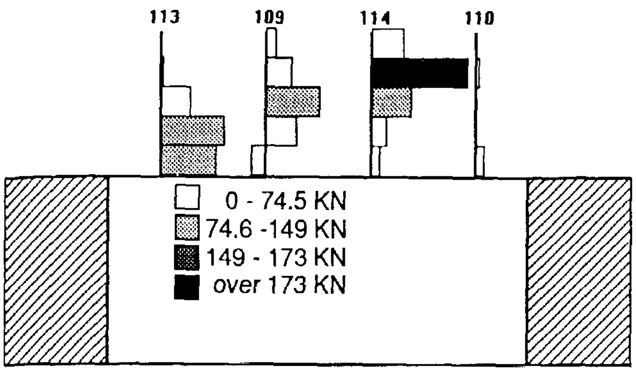

Figure 6.—Axial loads on test row 1 on 12/12/97

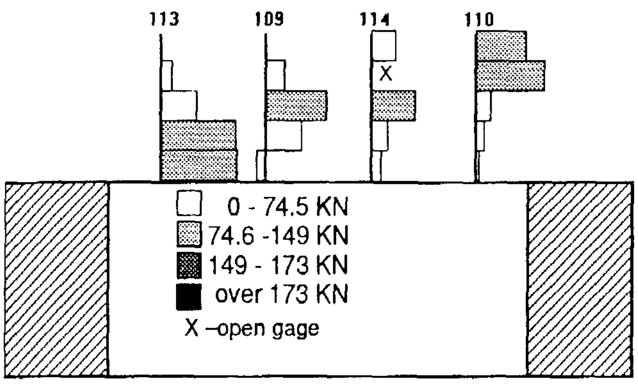

Figure 7.—Axial loads on test row 1 on 12/16/97

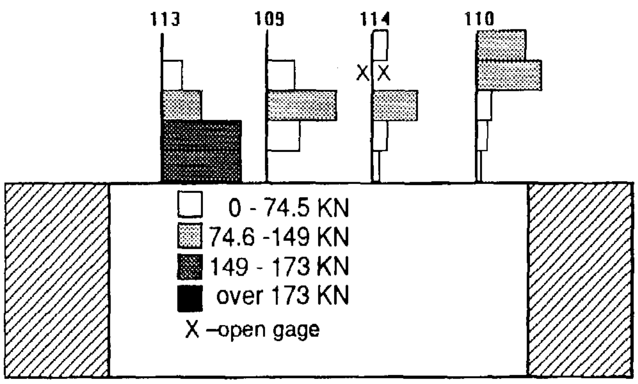

Figure 8.—Axial loads on test row 1 on 1/9/98

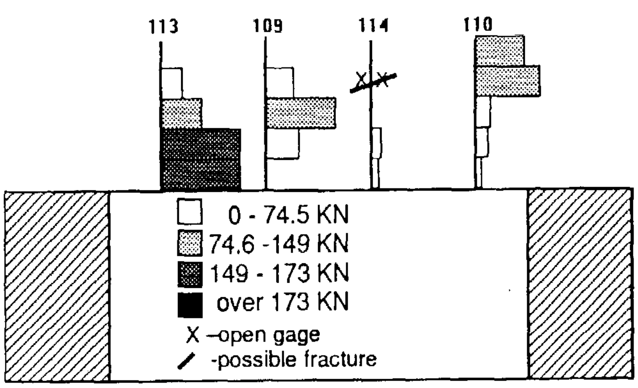

Figure 9.—Axial loads on test row 1 on 1/15/98

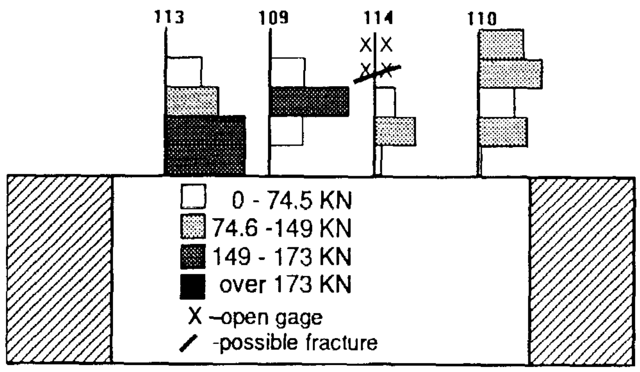

Figure 10.—Axial loads on test row 1 on 4/19/98

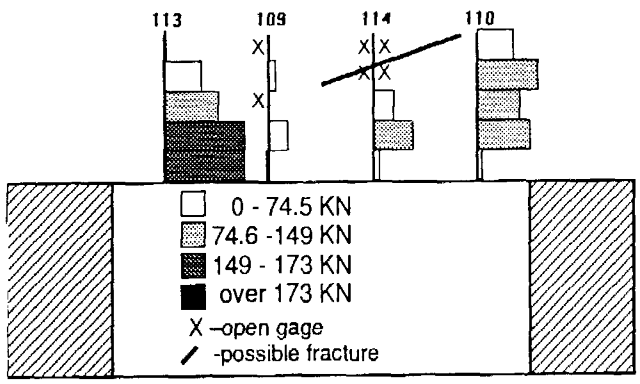

Figure 11.—Axial loads on test row 1 on 4/21/98

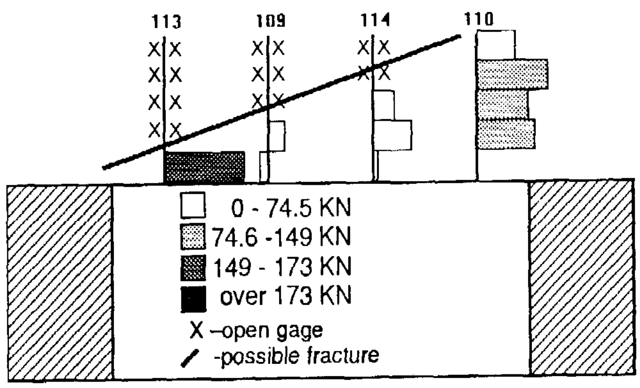

Figure 12.—Axial loads on test row 1 on 4/23/98

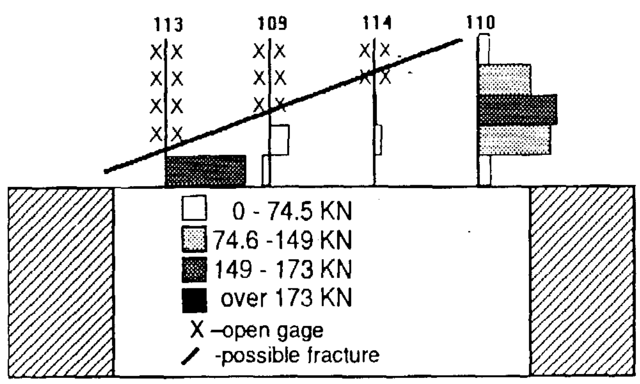

Figure 13.—Axial loads on test row 1 on 6/2/98

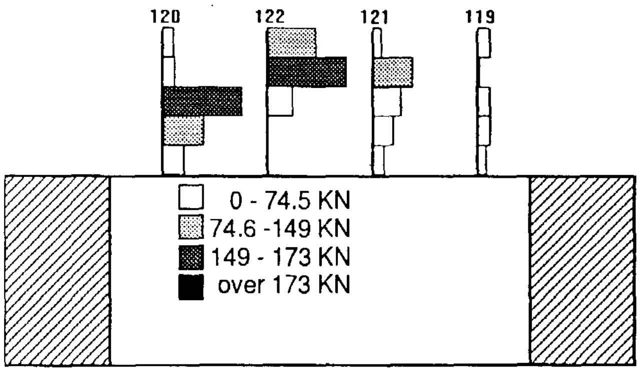

Figure 14.—Axial loads on test row 2 on 12/16/97

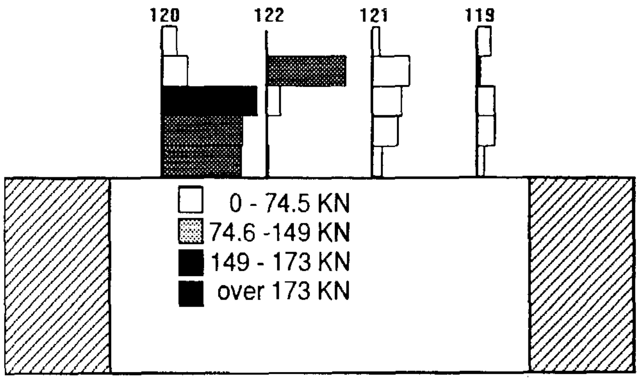

Figure 15.—Axial loads on test row 2 on 4/21/98

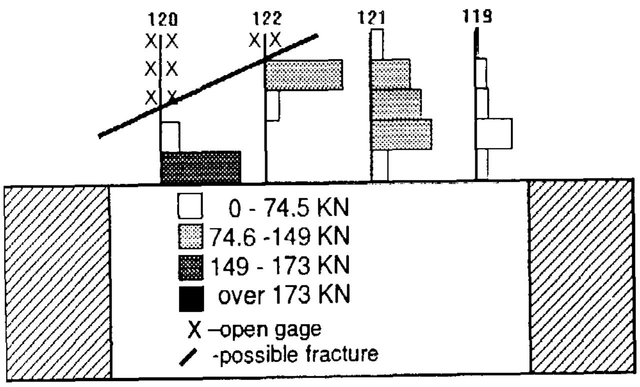

Figure 16.—Axial loads on test row 2 on 6/2/98

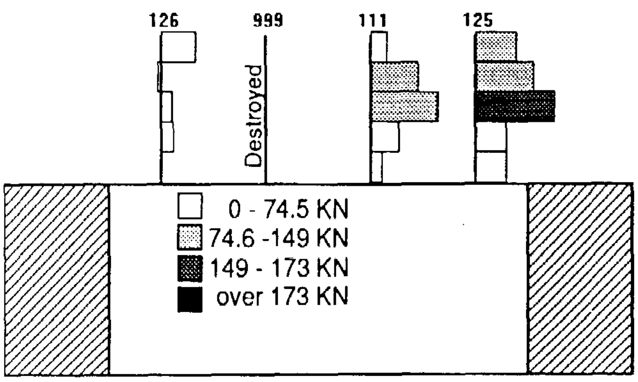

Figure 17.—Axial loads on test row 3 on 12/16/97

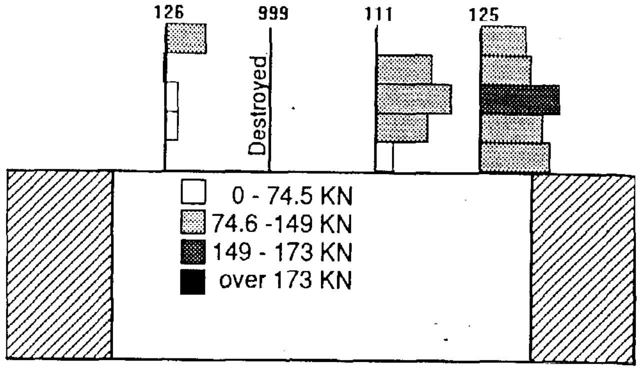

Figure 18.—Axial loads on test row 3 on 4/10/98

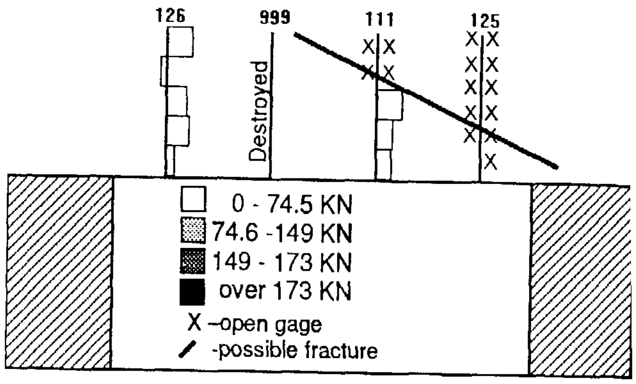

Figure19.—Axial loads on test row 3 on 6/2/98

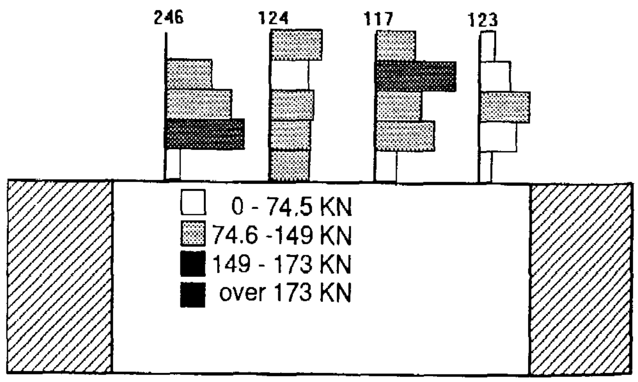

Figure 20.—Axial loads on test row 4 on 12/16/98

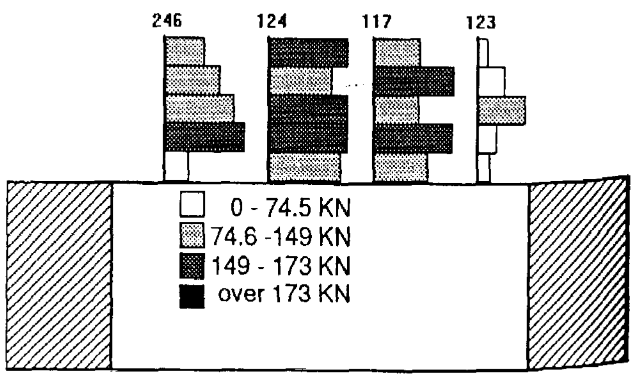

Figure 21.—Axial loads on test row 4 on 5/6/98

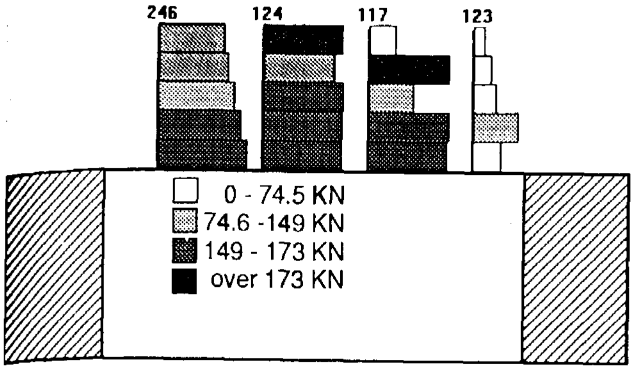

Figure 22.—Axial loads on test row 4 on 6/2/98

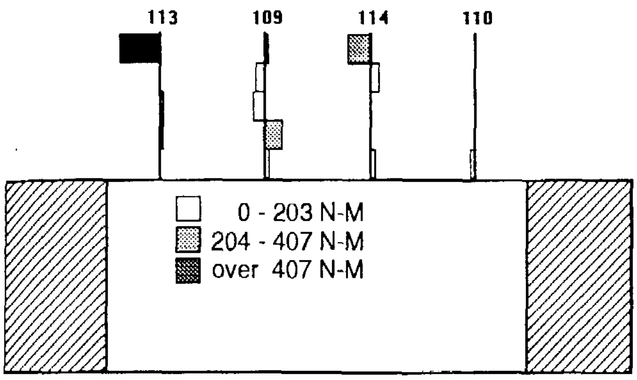

Figure 23.—Bending moments on test row 1 on 12/12/97

opposite gage 4 had an open reading. Six days later, the load level in bolt 114 dropped significantly, which may indicate that the bolt was beginning to break. On April 19, the last four gages were open, and loading increased in the adjacent bolts. Two days later, loading on adjacent bolt 109 dropped significantly and two open gages were recorded. Then on April 23, many of the strain gages had an open reading, which could have been caused by shear movement along a possible fracture plane (figure 13).

This sequence was repeated at test row 2, but only three time shots are shown. At this test site, the possible fracture plane was higher in the roof and affected only two instrumented bolts. A similar sequence was repeated at test row 3, but this time on the other side of the entry. In this test row, bolt 125 broke and was recovered on the mine floor. Test row 4 did not show any strain gage failures, and loading was more evenly distributed along the length of the bolts.

When a strain gage indicated an open reading, axial loading is not shown at that location because axial loading is an average of load on each side of the bolt. Open strain gages can be a result of either excessive loading or wire failure. Under axial loading, most lead wires maintain continuity until bolt failure. Recent shear tests on instrumented bolts show that lead wires are severed well in advance of bolt failure, and bending moments dissipate quickly from a shear joint. There are several indications that a bolt has broken: (1) high loads prior to failure, (2) loss of continuity to strain gages past the break, and (3) drop offs in loading in the bolt section before the break. Using these criteria, the data indicate that progressive bolt failure may have taken place in three of the four test rows.

Only one instrumented bolt had a maximum strain less than 2,000 microstrain, the yield point of the steel. The maximum strain of all of the bolts was 43,000 microstrain. The average maximum strain of each test area is shown in table 4.

Table 4.—Strain gage information

Row	Ave. max. strain, microstrain	Percentage of open gages	Percentage of broken bolts
1	18,600	45	75
2	20,500	20	50
3	22,100	46	66
4	18,800	0	0

Microstrain is not a good measure of support effectiveness in each test area because so many of the bolts failed. A better measure is the percentage of strain gages and bolts that failed. The highest percentage of gage failures was in test row 1 and test row 3. The lowest percentage of gage failures was in test row 4.

When comparing load values among test areas it is important to remember that fully grouted cables have a higher ultimate strength than resin bolts. On the other hand, fully grouted cables have less ductility. Also, fully grouted cable bolts are larger in diameter than partly grouted cables and have a higher load capacity. The instrumented resin bolts had more cross-sectional area than the unslotted resin bolts. This means that the ordinary resin bolts probably failed before the instrumented bolts.

A typical plot of the bending moments is shown in figure 23. If shear forces caused by joint planes were the primary means of bolt failure, then the bending moments would be very localized and might not be detected because of the large spacing of the strain gages. Resin bolts will not fail under pure bending because of the high ductility of the steel. For this reason, axial loads are a better indicator of bolt failure.

Loading on the cable bolts in test rows 1 and 2 is shown in figure 24. Loading was fairly low until the abutment stress from the longwall panel approached the test areas, at which time the load increased rapidly and the pressure pads failed to work on all but cable 3. Several uninstrumented cables broke in both test areas along with instrumented cable 4.

The amount of deflection measured in test row 2 is shown in table 5. By December 12, 5 mm (0.197 in) of movement had taken place within the upper end of the bolted zone. This was enough movement to load a fully grouted bolt to the yield point of the steel (bolt 122 located next to the sagmeter hole). By June 2, 111 mm (4.37 in) of movement had occurred in this same zone, which was enough movement to cause the bolt to break. Very little movement was recorded in any other zones in this sagmeter hole.

Table 5.—Amount of roof deflections in test row 2, millimeters

Distance from roofline, m	Date		
	12/16/97	4/19/98	6/2/98
3 to 4.3	1	4	3
1.8 to 3	0	2	1
0.9 to 1.8	5	13	111
0 to 0.9	0	2	-5

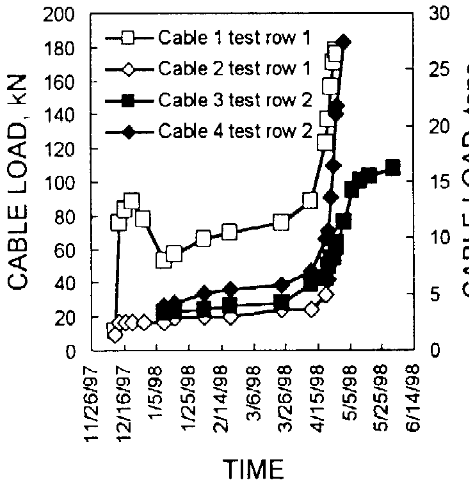

Figure 24.—Cable bolt loads

DISCUSSION

All data showed that enough movement was taking place within the bolted zone to load the supports past ultimate strength. Behavior of the strain gages indicated that shear forces added to axial loading caused bolt failure. The weak mudstone layer and the very strong siltstone-sandstone layer were significant factors because of their great difference in rock strength. By itself, the weight of the material was not enough to produce the bolt loads measured. However, weak material could dilate over the pillars and cause horizontal forces that would exceed the strength of the weaker material. This could have produced tensile failures in the rock that created shear forces on the supports.

Another possibility is that when the yield pillar deformed, the weaker mudstone developed shear cracks similar to those seen in short concrete beam failures. The true cause could be a combination or none of these factors. Observations in this area uncovered more problems at mid-pillar locations than at intersections. This could be caused by the dilation effect of yielding pillars. The wire mesh and concrete cans installed as secondary support were very effective, given the roof conditions.

REFERENCES

1. Signer, S. P., and S. D. Jones. A Case Study of Grouted Roof Bolt Loading in A Two-Entry Gate Road. Paper in *9th International Conference on Ground Control in Mining: Proceedings*, ed. by Syd S. Peng (Morgantown, WV, June 4-10, 1990). Dept. of Mining Engineering, WV Univ., 1990, pp. 35-41.

2. Signer, S. P., C. Mark, G. Franklin, and G. Hendon. Comparisons of Active Versus Passive Bolts in a Bedded Mine Roof. Paper in *Proceedings of 12th Conference on Ground Control in Mining*, ed. by S. S. Peng (Morgantown, WV., Aug. 3-5, 1993). Dept. of Mining Engineering, WV Univ., 1993, pp. 16-23.

3. Signer, S. P. Field Evaluations of Grouted Roof Bolts. In *New Technology for Longwall Ground Control. Proceedings: U.S. Bureau of Mines Technology Transfer Seminar*, comp. by C. Mark, R. J. Tuchman, R. C. Repshar, and C. L. Simon. U.S. Bur. Mines Spec. Pub. 01-94, 1994, pp. 91-101.

4. Serbousek, M. O., and S. P. Signer. Load Transfer Mechanics in Fully Grouted Roof Bolts. Paper in *Proceedings, Fourth Conference on Ground Control in Mining* (Morgantown, WV, July 22-24, 1985). Dept. of Mining Engineering, WV Univ.,1985, pp. 32-40.

5. Serbousek, M. O., and S. P. Signer. Linear Load Transfer Mechanics of Fully-Grouted Bolts. U.S. Bur. Mines RI 9135, 1987, 17 pp.

6. Maleki, H., S. P. Signer, M. E. King, and P. A. Edminster. Evaluation of Support Performance in a Highly Stressed Mine. Paper in *Proceedings of 13th International Conference on Ground Control in Mining*, ed. by S. S. Peng (Morgantown, WV, Aug. 2-4, 1994). Dept. of Mining Engineering, WV Univ., Morgantown, WV, 1994, pp. 9-17.

7. Larson, M., C. Stewart, M. Stevenson, M. King, and S. Signer A Case Study of a Deformation Mechanism Around a Two-Entry Gateroad System Involving Probable Time-Dependent Deformation. Paper in *Proceedings of 14th International Conference on Ground Control in Mining*, ed. by S. S. Peng (Morgantown, WV, Aug. 1-3, 1995). Dept. of Mining Engineering, WV Univ., 1995, pp. 295-304.

8. Farmer, I. W. Stress Distribution Along a Resin Grouted Anchor. *Int. J. Rock Mech. Min. Sci. & Geomech*, v. 12, 1975, pp. 347-351

9. Dunham, R. K. Anchorage Tests on Strain-Gaged Resin Bonded Bolts. *Tunnels and Tunneling*, v. 8, No. 6. Sept. 1974, pp. 73-76.

10. Gale, W. J., and M. W. Fabjanczyk. Application of Field Measurement Techniques to the Design of Roof Reinforcement Systems in Underground Coal Mines. Paper in Proceedings, 13th Congress of Council of Inst. Min. and Metal., Singapore, pp. 135-141.